

S-ACOT Heavy flavor contributions at NNLO in CTEQ-TEA analysis

Marco Guzzi

Southern Methodist University

Winter Workshop on Recent QCD Advances at the LHC
Les Houches, February 13th - 18th, 2011

In collaboration with P. Nadolsky, C.-P. Yuan and H.L. Lai

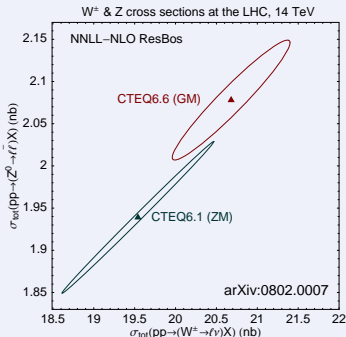
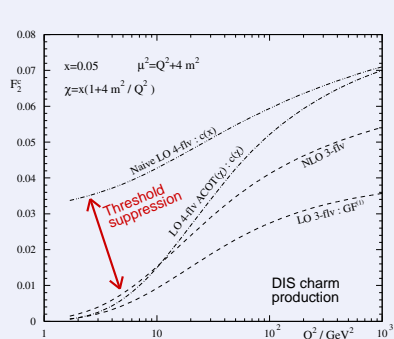


Heavy-quark DIS and LHC observables

Motivation:

General-mass (and not zero-mass of fixed-flavor number) treatment of c , b mass terms in DIS is essential for predicting precision W , Z cross sections at the LHC (*Tung et al., hep-ph/0611254*)

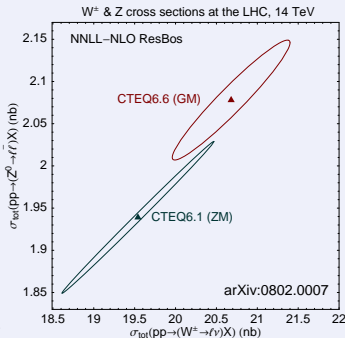
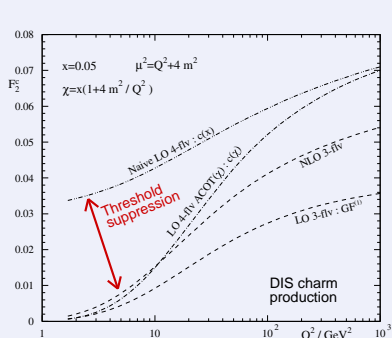
Several quark mass effects are comparable to NNLO radiative contributions, must be included in a consistent way



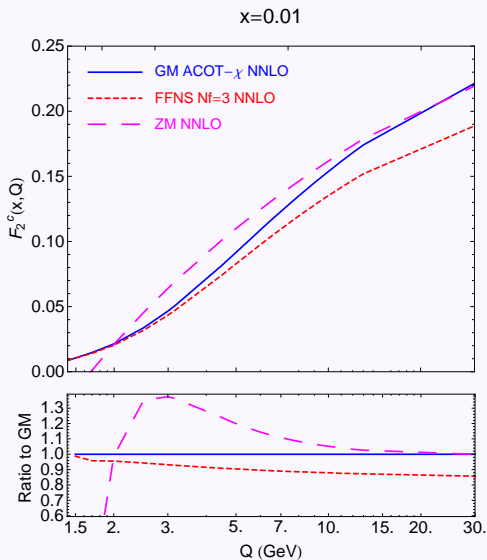
Heavy-quark DIS and LHC observables

This talk:

- an NNLO computation for heavy-quark DIS structure functions, $F_i^{c,b}(x, Q)$, in a general-mass scheme (S-ACOT)
- focus on consistent treatment of all relevant factors in $F_i^{c,b}(x, Q)$ affecting CTEQ-TEA PDFs at NNLO accuracy



$F_2^c(x, Q^2)$ at NNLO - Preliminary

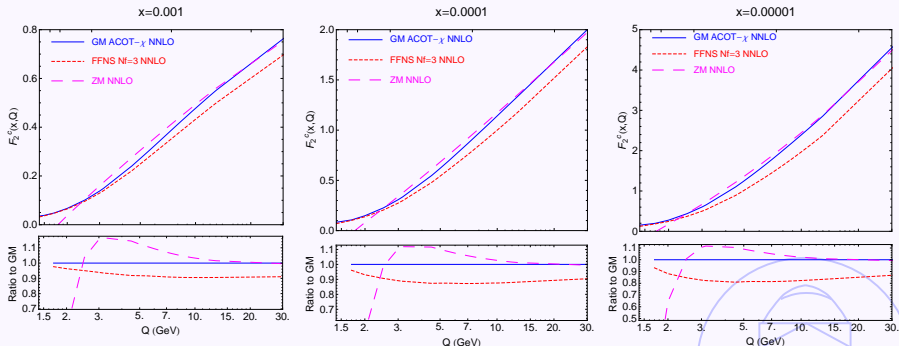


S-ACOT reduces
to FFNS at $Q \approx m_c$
and to ZM at $Q \gg m_c$

Les Houches toy
PDFs, evolved at
NNLO with
threshold matching
terms

NNLO predictions for
 F_L^c are in the backup
slides

$F_2^c(x, Q^2)$ at NNLO, other x bins - Preliminary



Simplified Aivazis-Collins-Olness-Tung scheme

ACOT, PRD 50 3102 (1994); Collins, PRD 58 (1998) 094002; Kramer, Olness, Soper, PRD (2000) 096007

- The default mass scheme of CTEQ6.6 and CT10 PDFs
- Based upon, and closely follows, the proof of QCD factorization for DIS with massive quarks (*Collins, 1998*)
- Relatively simple, compared to BMSN or TR schemes
 - ▶ One value of N_f (and one PDF set) in each Q range
 - ▶ Straightforward matching based on kinematical rescaling
 - ▶ Sets $m_Q = 0$ in ME with incoming c or b
- Reduces to the ZM \overline{MS} scheme at $Q^2 \gg m_Q^2$, without additional renormalization
- Reduces to the FFN scheme at $Q^2 \approx m_Q^2$
 - ▶ has reduced dependence on tunable parameters at NNLO



S-ACOT input parameters

At $Q \approx m_c$, F_2^c depends significantly on

1. **Charm mass:** $m_c = 1.3$ GeV in CT10
2. **Factorization scale:** $\mu = \sqrt{Q^2 + \kappa m_c^2}$; $\kappa = 1$ in CT10
3. **Rescaling variable** $\zeta(\lambda)$ for matching in γ^*c channels

(Tung et al., hep-ph/0110247; Nadolsky, Tung, PRD79, 113014 (2009))

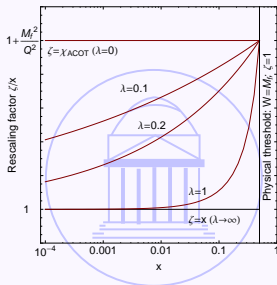
$$F_i(x, Q^2) = \sum_{a,b} \int_{\zeta}^1 \frac{d\xi}{\xi} f_a(\xi, \mu) C_{b,\lambda}^a \left(\frac{\zeta}{\xi}, \frac{Q}{\mu}, \frac{m_i}{\mu} \right)$$

$$x = \zeta / \left(1 + \zeta^\lambda \cdot (4m_c^2)/Q^2 \right), \text{ with } 0 \leq \lambda \lesssim 1$$

CT10 uses

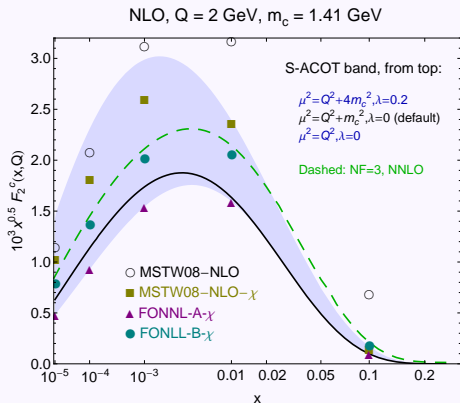
$$\zeta(0) \equiv \chi \equiv x \left(1 + 4m_c^2/Q^2 \right),$$

motivated by momentum conservation



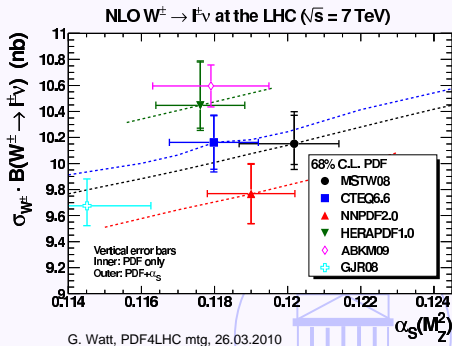
Input parameters of the S-ACOT scheme

At NLO, the m_c , μ , and ζ parameters of CTEQ PDFs are tuned to best describe the DIS data



2009 Les Houches HQ benchmarks with toy PDFs:

$\mu = Q$ in non-CTEQ predictions

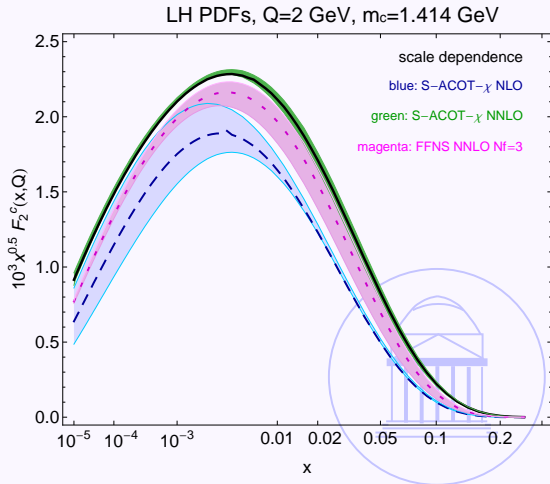


W, Z cross sections;
 $m_c = 1.3 \text{ GeV}$ in CTEQ6.6

Results for $F_2^c(x, Q^2)$ at NLO/NNLO - Preliminary

At NNLO and $Q \approx m_c$:

■ S-ACOT- $\chi \approx$ FFN($N_f = 3$)
without tuning

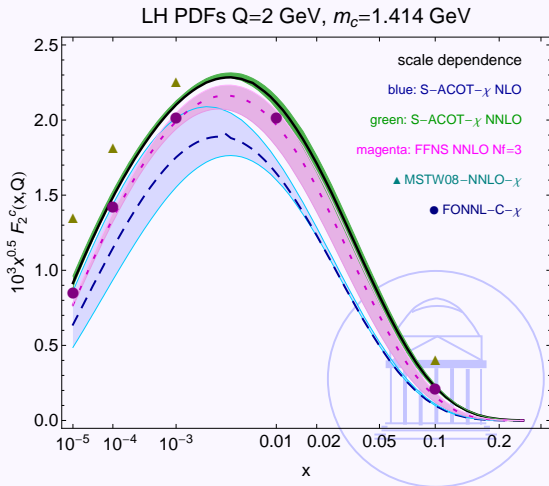


Results for $F_2^c(x, Q^2)$ at NLO/NNLO - Preliminary

At NNLO and $Q \approx m_c$:

■ S-ACOT- $\chi \approx$ FFN($N_f = 3$)
without tuning

■ It is close to other NNLO
schemes



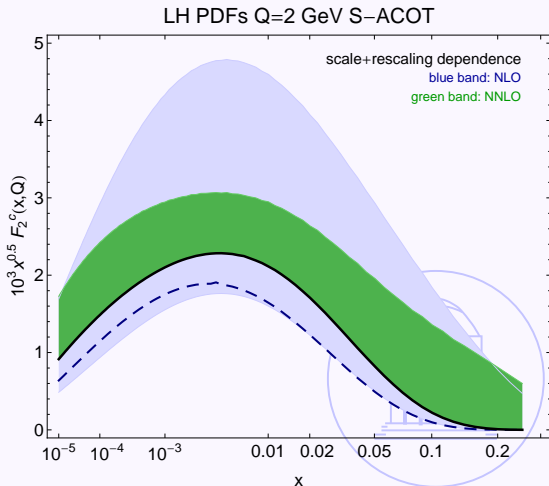
Results for $F_2^c(x, Q^2)$ at NLO/NNLO - Preliminary

At NNLO and $Q \approx m_c$:

■ S-ACOT- $\chi \approx$ FFN($N_f = 3$)
without tuning

■ It is close to other NNLO schemes

■ Dependence on rescaling is also reduced

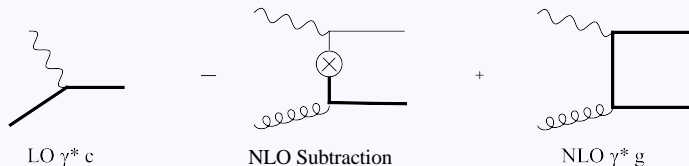


Details of the computation

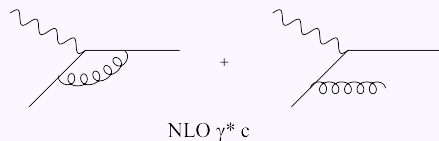
- NNLO evolution for α_s and PDFs (HOPPET)
 - ▶ matching coefficients relating the PDFs in N_f and N_{f+1} schemes (*Smith, van Neerven, et al.*)
- NNLO Wilson coefficient functions for $F_2^c(x, Q)$, $F_L^c(x, Q)$
- Work in progress: \overline{MS} masses from PDG as input



Classes of Feynman diagrams I

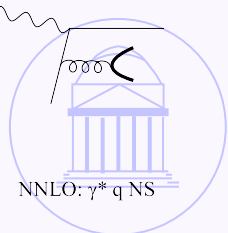
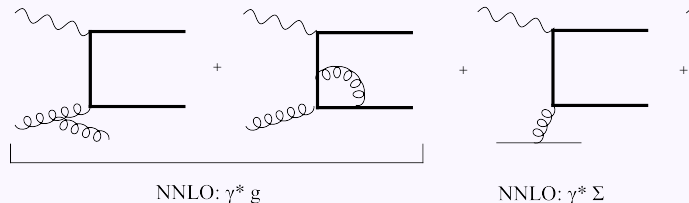


ACOT II: Phys.Rev.D50 (1994) 3102



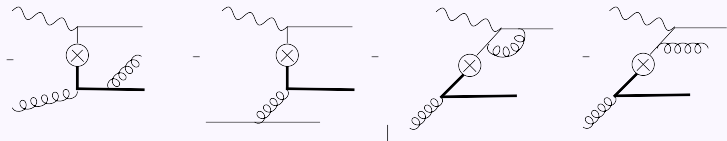
Furmanski, Petronzio, Z.Phys. C11 (1982) 293.

Kramer, Olness, Soper, PR D62 (2000) 096007



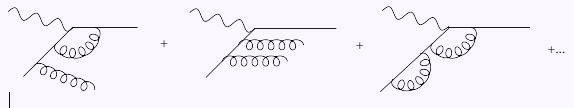
Riemersma et. al. Phys.Lett. B347 (1995) 143

Classes of Feynman Diagrams II



NNLO Subtractions

Buza, Matiounine, Smith, Van Neerven, Eur. Phys. J. C 1998



NNLO $\gamma^* c$

Moch, Vermaseren and Vogt, Nucl.Phys.B724, 2005



Cancellations between Feynman diagrams

Validity of the S-ACOT calculation was verified by checking for certain cancellations at $Q \approx m_c$ and $Q \gg m_c$

■ $Q \approx m_c$:

$$D_{C1}^{(2)} \ll D_{C0}^{(2)} \ll D_{C0}^{(1)} \leq F_2^c(x, Q)$$

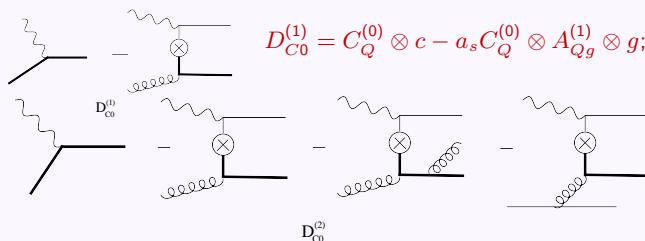
■ $Q \gg m_c$:

$$D_g^{(2)} \ll D_g^{(1)} < F_2^c(x, Q)$$

These cancellations are indeed observed in our results

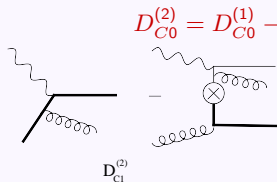


NNLO: Cancellations at $Q^2 \approx m_c^2$



Diagrammatic representation of $D_{C_0}^{(1)}$ showing four terms. Each term consists of a hard scattering process (represented by a vertex with a cross) and a soft function (represented by a gluon line). The terms are: 1) a gluon line from the hard vertex to the left; 2) a gluon line from the hard vertex to the right; 3) a gluon line from the hard vertex to the bottom; 4) a gluon line from the hard vertex to the top.

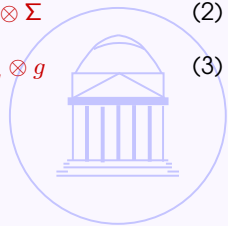
$$D_{C_0}^{(1)} = C_Q^{(0)} \otimes c - a_s C_Q^{(0)} \otimes A_{Qg}^{(1)} \otimes g; \quad a_s = \frac{\alpha_s}{(4\pi)} \quad (1)$$



Diagrammatic representation of $D_{C_1}^{(2)}$ showing two terms. Each term consists of a hard scattering process (represented by a vertex with a cross) and a soft function (represented by a gluon line). The terms are: 1) a gluon line from the hard vertex to the left; 2) a gluon line from the hard vertex to the right.

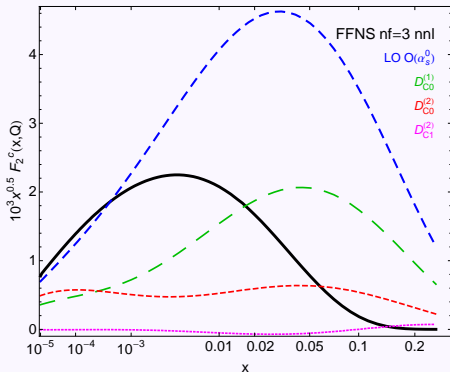
$$D_{C_0}^{(2)} = D_{C_0}^{(1)} - a_s^2 C_Q^{(0)} \otimes A_{Qg}^{(2),S} \otimes g - a_s^2 C_Q^{(0)} \otimes A_{Q\Sigma}^{(2),PS} \otimes \Sigma \quad (2)$$

$$D_{C_1}^{(2)} = C_Q^{(1)} \otimes c - a_s^2 C_Q^{(1)} \otimes A_{Qg}^{(1)} \otimes g \quad (3)$$

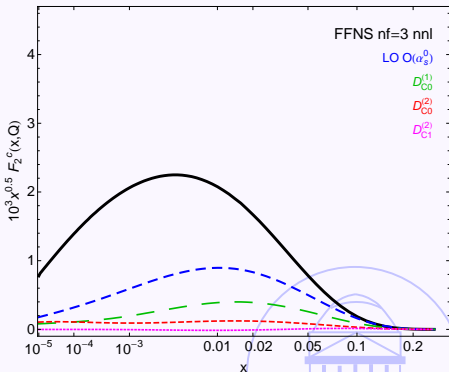


NNLO: Cancellations at $Q^2 \approx m_c^2$

LH PDFs $Q=2$ GeV Acot- X $\zeta=x$

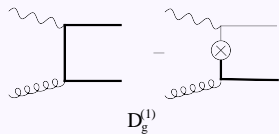


LH PDFs $Q=2$ GeV Acot- X $\zeta=\chi$



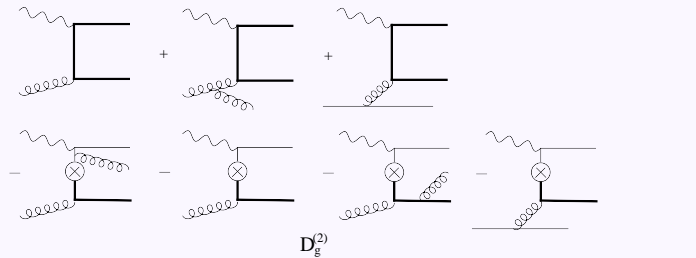
$D_{C1}^{(2)} \ll D_{C0}^{(2)} \ll D_{C0}^{(1)} \leq$ FFN at NNLO both for $\zeta = x$ and $\zeta = \chi$.

NNLO: Cancellations at $Q \gg m_c$



Diagrammatic representation of $D_g^{(1)}$: a box diagram with a gluon line on the left and a quark line on the top, minus a diagram with a quark loop on the top and a gluon line on the left.

$$D_g^{(1)} \equiv C_g^{(1)} = a_s \left(F_g^{(1)} \otimes g - C_Q^{(0)} \otimes A_{Qg}^{(1),S} \otimes g \right) \quad (4)$$



Diagrammatic representation of $D_g^{(2)}$: a sum of seven diagrams. The first three are box diagrams with different gluon line attachments. The last four are diagrams with quark loops and various gluon line attachments.

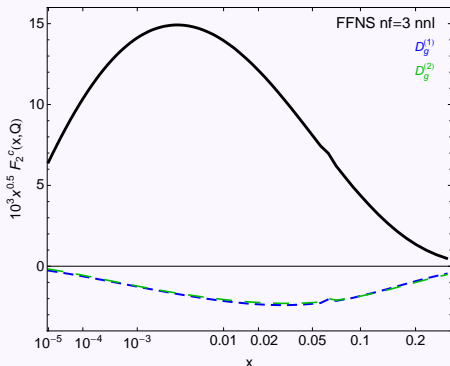
$$D_g^{(2)} = D_g^{(1)} + a_s^2 \left[\tilde{F}_g^{(2)} \otimes g + \tilde{F}_\Sigma^{(2)} \otimes \Sigma - C_Q^{(1)} \otimes A_{Qg}^{(1),S} \otimes g - C_Q^{(0)} \otimes A_{Qg}^{(2),S} \otimes g - C_Q^{(0)} \otimes A_{Q\Sigma}^{(2),PS} \otimes \Sigma \right] \quad (5)$$

$D_g^{(1)}$ is of order of α_s^2 while $D_g^{(2)}$ is of order of α_s^3 .

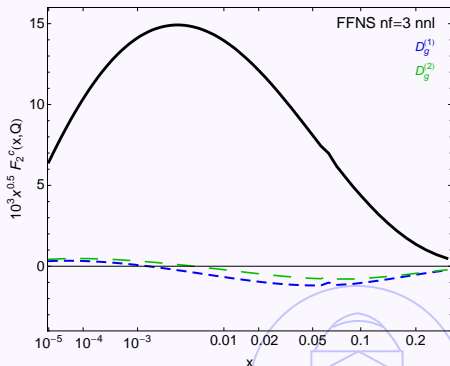


F_2^c at NNLO: Cancellations at $Q = 10 \text{ GeV}$

LH PDFs $Q=10 \text{ GeV}$ Acot-X $\zeta=x$

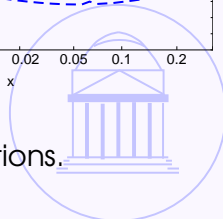


LH PDFs $Q=10 \text{ GeV}$ Acot- χ $\zeta=\chi$



$D_g^{(2)} \ll D_g^{(1)} < \text{FFN at NNLO} < \text{ACOT}$

$\log \frac{Q^2}{m_c^2}$ terms in FFN are cancelled well by subtractions.



Main messages

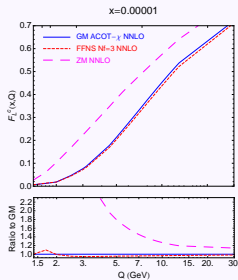
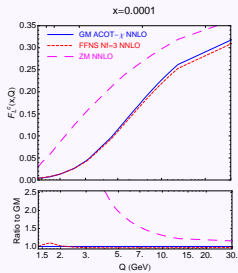
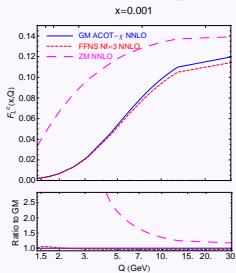
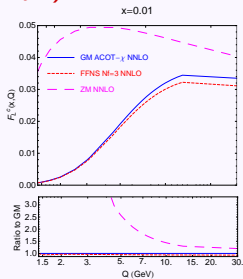
- An NNLO calculation for $F_2^{c,b}$ and $F_L^{c,b}$ in the S-ACOT scheme is proven to be viable
- This is the most challenging component of the NNLO CTEQ PDF analysis, which will be made available soon.
- NNLO predictions are stable and show a remarkable reduction in the dependence on free parameters, compared to NLO.
- They will help us to reduce tuning of m_c and scale parameters, currently used by NLO CT10 PDFs to achieve excellent agreement with the HERA DIS data



BACK UP SLIDES



$F_L^c(x, Q^2)$ at NNLO - Preliminary

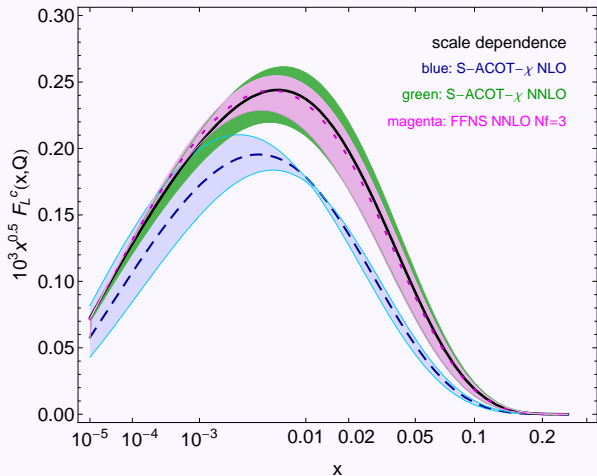


S-ACOT is close to FFNS at all Q .
ZM overestimates S-ACOT everywhere



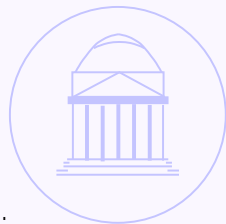
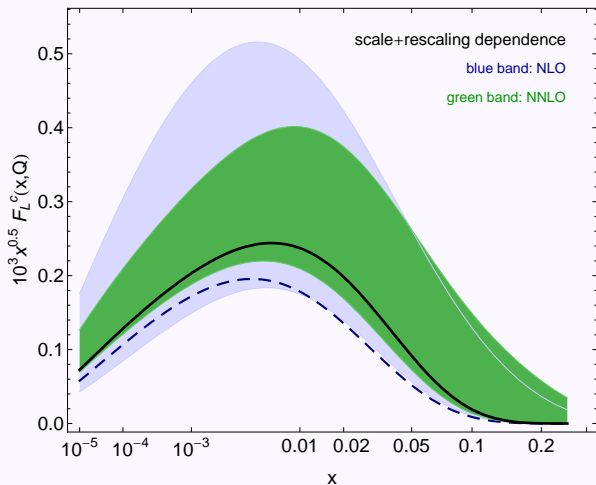
Results for $F_L^c(x, Q^2)$ at NLO/NNLO - Preliminary

LH PDFs Q=2 GeV



Results for $F_L^c(x, Q^2)$ at NLO/NNLO - Preliminary

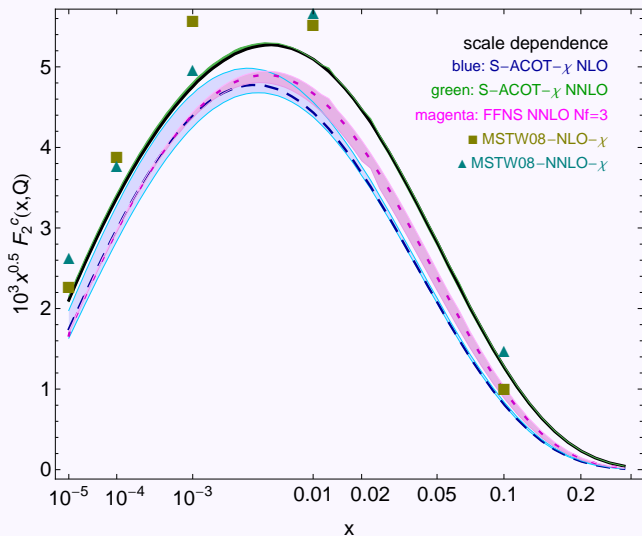
LH PDFs $Q=2$ GeV S-ACOT



Plots for $Q^2 = 10 \text{ GeV}^2$ and $Q^2 = 100 \text{ GeV}^2$ are in the backup.

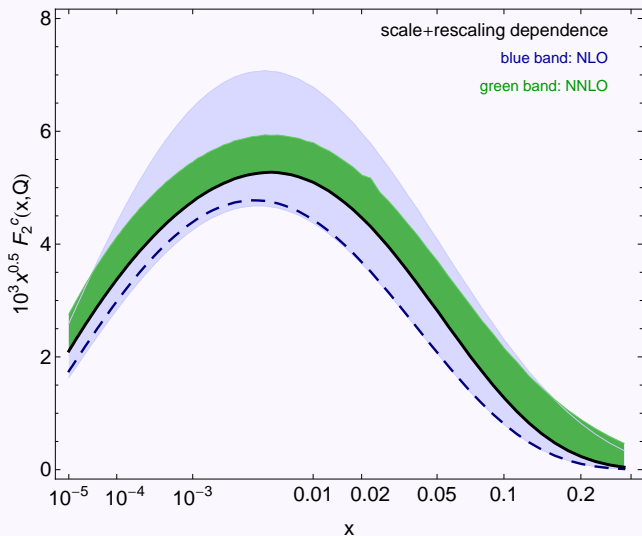
Results for $F_2^c(x, Q^2)$ at NLO/NNLO - Preliminary

LH PDFs $Q=3.162$ GeV



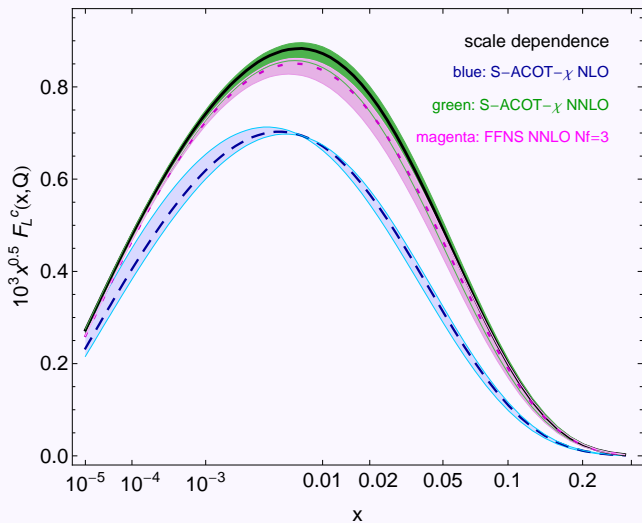
Results for $F_2^c(x, Q^2)$ at NLO/NNLO - Preliminary

LH PDFs $Q=3.162$ GeV S-ACOT



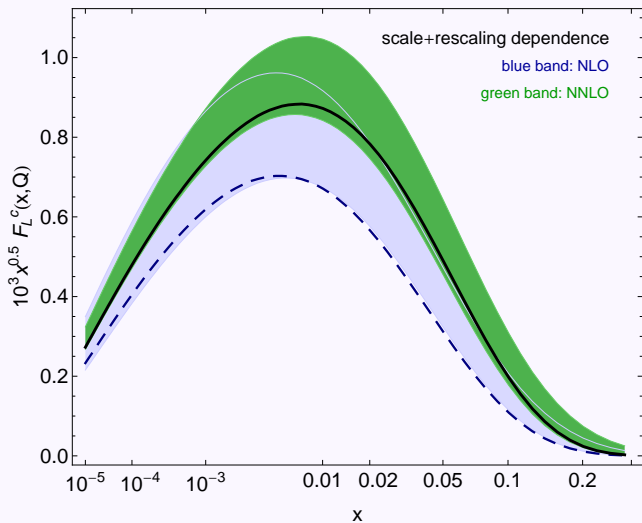
Results for $F_L^c(x, Q^2)$ at NLO/NNLO - Preliminary

LH PDFs $Q=3.162$ GeV

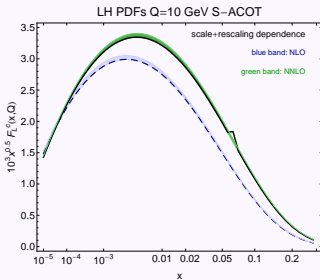
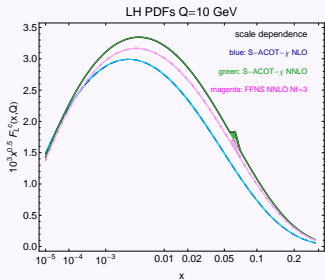
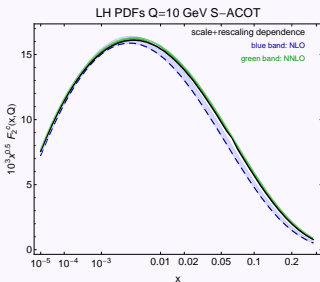
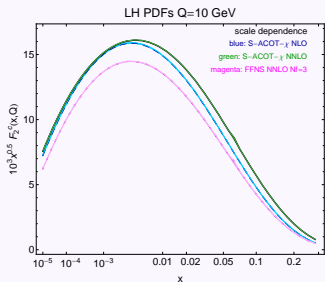


Results for $F_L^c(x, Q^2)$ at NLO/NNLO - Preliminary

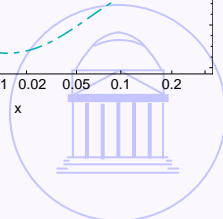
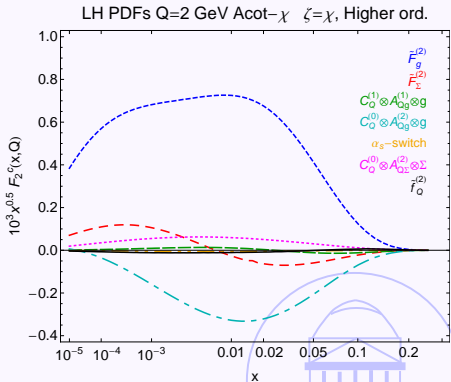
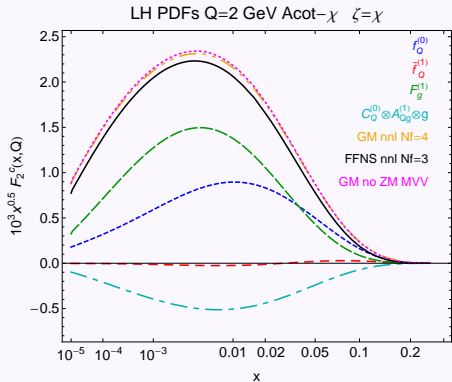
LH PDFs $Q=3.162$ GeV S-ACOT



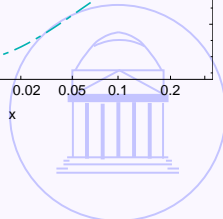
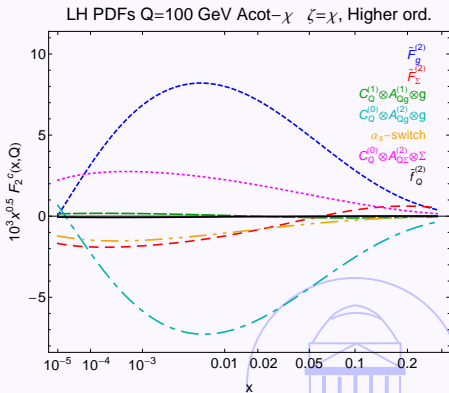
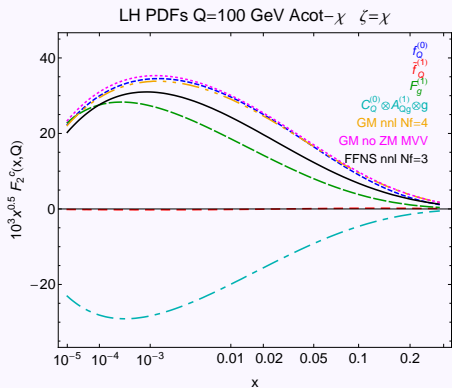
$F_{2,L}^c(x, Q^2)$ at NLO/NNLO $Q = 10$ GeV - Preliminary



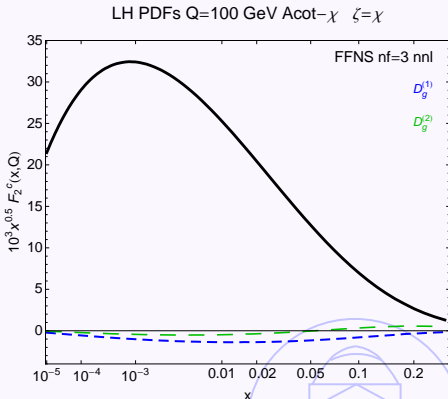
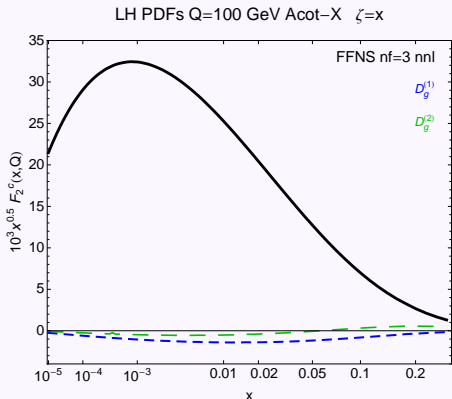
F_2^c : Anatomy of the contributions $Q = 2 \text{ GeV}$



F_2^c : Anatomy of the contributions $Q = 100 \text{ GeV}$

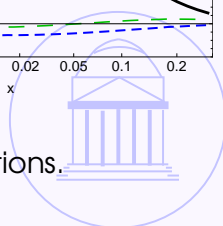


F_2^c at NNLO: Cancellations at $Q = 100 \text{ GeV}$



$D_g^{(2)} \ll D_g^{(1)} < \text{FFN at NNLO} < \text{Acot}$

$\log \frac{Q^2}{m_c^2}$ terms in FFN are cancelled well by subtractions.



FNFS expression for $F_{2,L}^c(x, Q)$

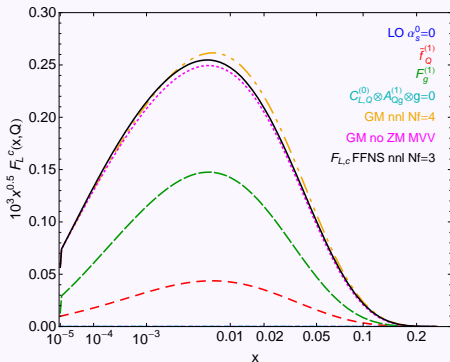
- Riemersma, Smith, Van Neerven, Phys. Lett. B347 (1995)
143-151- The structure functions are given by

$$\begin{aligned} F_k(x, Q) &= \frac{Q^2 \alpha_s}{4\pi^2 m^2} \int_x^{z_{max}} \frac{dz}{z} \left[e_H^2 g\left(\frac{x}{z}, \mu^2\right) c_{k,g}^{(0)} \right] \\ &+ \frac{Q^2 \alpha_s^2}{\pi m^2} \int_x^{z_{max}} \frac{dz}{z} \left\{ e_H^2 g\left(\frac{x}{z}, \mu^2\right) \left(c_{k,g}^{(1)} + \bar{c}_{k,g}^{(1)} \ln \frac{\mu^2}{m^2} \right) \right. \\ &+ \sum_{i=q, \bar{q}} \left[e_H^2 f_i\left(\frac{x}{z}, \mu^2\right) \left(c_{k,i}^{(1)} + \bar{c}_{k,i}^{(1)} \ln \frac{\mu^2}{m^2} \right) \right. \\ &+ \left. \left. e_{L,i}^2 f_i\left(\frac{x}{z}, \mu^2\right) \left(d_{k,i}^{(1)} + \bar{d}_{k,i}^{(1)} \ln \frac{\mu^2}{m^2} \right) \right] \right\}, \end{aligned} \quad (6)$$

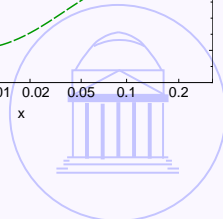
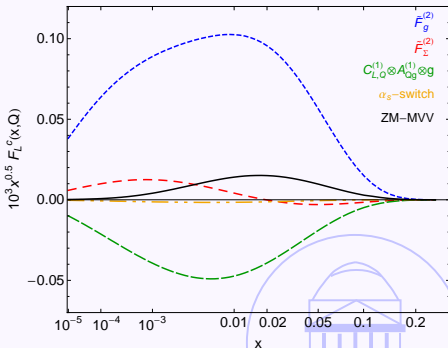
Here e_H is the charge of the heavy quark while e_L refers to the light quark. Furthermore $k = 2, L$, $z_{max} = Q^2 / (Q^2 + 4m^2)$ and $i = g, q, \bar{q}$.

$F_{L,c}^c$: Anatomy of the contributions $Q = 2 \text{ GeV}$

LH PDFs $Q=2 \text{ GeV}$ Acot- χ $\zeta=\chi$

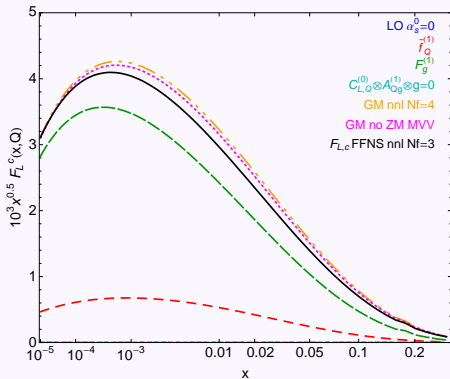


LH PDFs $Q=2 \text{ GeV}$ Acot- χ $\zeta=\chi$, Higher ord.



F_L^c : Anatomy of the contributions $Q = 100 \text{ GeV}$

LH PDFs $Q=100 \text{ GeV}$ Acot- χ $\zeta=\chi$



LH PDFs $Q=100 \text{ GeV}$ Acot- χ $\zeta=\chi$, Higher ord.

